Coarse Graining in Micromagnetics

G. Grinstein and R. H. Koch

IBM T. J. Watson Research Center, P.O. Box 218, Yorktown Heights, New York 10598, USA

(Received 25 January 2002; published 19 May 2003)

Numerical solutions of the micromagnetic Landau-Lifshitz-Gilbert equations provide valuable information at low temperatures (T), but produce egregious errors at higher T. For example, Curie temperatures are often overestimated by an order of magnitude. We show that these errors result from the use of block or coarse-grained variables, without a concomitant renormalization of the system parameters to account for the block size. Renormalization solves the problem of the Curie-point anomaly and improves the accuracy of more complicated micromagnetic simulations, even at low T.

DOI: 10.1103/PhysRevLett.90.207201 PACS numbers: 75.50.Tt, 05.40.–a, 75.40.Cx, 75.40.Mg

Numerical simulation of complex classical magnetic systems has become an essential tool in the remarkably successful effort [1] to increase the speed and capacity of magnetic storage devices. While most such simulations have been performed at zero temperature, where the micromagnetic equations of Landau and Lifshitz (LL) [2] or, equivalently [3], of Gilbert (G) [4], constitute a reliable starting point, the decreasing size of magnetic devices makes thermal fluctuations so large that simulations purporting to be realistic must often include them. Brown [5] has provided a prescription for adding thermal noise to the LLG equations so as to ensure that in the long-time limit the system achieves the stationary Boltzmann distribution for the energy function describing the magnetic interactions. In principle, this allows accurate numerical simulations of magnetic devices at nonzero temperature, $\tilde{T}$. In practice, however, simulations that work well for $\tilde{T}$ far below the Curie temperature, $\tilde{T}_c$, produce surprisingly bad results closer to $\tilde{T}_c$. In particular, they overestimate $\tilde{T}_c$ itself by factors of 5 to 10 or more [6].

In this Letter, we argue that this difficulty is one of coarse graining: It is too expensive computationally to carry out simulations on the microscopic level of individual spins. Rather, simulators use block or coarse-grained spins as their basic variables. However, this requires special care to be paid to how the parameters of the system vary with the block size. Such analysis is of course precisely what the renormalization group (RG) was designed to accomplish. Accordingly, in the first part of this paper we show that the problem of overestimated Curie temperatures can be solved by an appeal to the low-temperature renormalization of fixed-length spin models [7,8]. The main point is that the effective exchange constant of the coarse-grained system experiences a *temperature-dependent* renormalization, thereby producing a phase transition at the proper temperature.

In the second part of the paper, we show that even at temperatures far below criticality, magnetic properties computed numerically from the LLG equations depend on block size. Using the RG, we estimate this dependence, verifying the predictions with explicit LLG calculation for the particular example of equilibrium M vs H curves in a simple model. Thus the RG is shown to provide a prescription for choosing the parameters as a function of block size in a general LLG computation.

The noisy LL equation for a classical magnetic moment vector field [9], $\vec{S}(\vec{x}, t)$, of fixed magnitude, S is

$$\frac{\partial \vec{S}(\vec{x}, t)}{\partial t} = \gamma \vec{S} \times \frac{\delta E(\{\vec{S}\})}{\delta \vec{S}(\vec{x})} + \alpha\gamma \hat{s} \times \left(\vec{S} \times \frac{\delta E(\{\vec{S}\})}{\delta \vec{S}(\vec{x})} \right) + \vec{S} \times \vec{\eta}(\vec{x}, t). \tag{1}$$

Here $\gamma = 1.76 \times 10^{11}$ C/kg is the gyromagnetic ratio, α is the dimensionless damping constant, $\hat{s} \equiv \vec{S}/S$, and the energy functional $E(\{\vec{S}\})$ describes the total energy of the system. The first two terms on the right side of (1) respectively represent the precession of magnetic moments around their local magnetic fields, $-\delta E(\{\vec{S}\})/\mu_0 \delta \vec{S}(\vec{x})$, (with μ_0 the vacuum permeability), and the simultaneous relaxation of the system towards lower energy. The final term represents random noise. If the strength, D, of the Gaussian random noise variable, $\vec{\eta}(\vec{x}, t)$, with correlations $\langle \eta_i(\vec{x}, t) \eta_j(\vec{x}', t') \rangle = D\delta_{ij}\delta \times (\vec{x} - \vec{x}')\delta(t - t')$, satisfies $D = 2k_B \tilde{T} \alpha\gamma/|\vec{S}|$, then, in the long-time limit, and independent of the values of α and γ, the system achieves the equilibrium Boltzmann distribution for the energy $E(\{\vec{S}\})$ at temperature $\tilde{T}$ [10].

By taking the dot product of (1) with $\vec{S}$, it is easily verified that Eq. (1) preserves the spin magnitude at each point in space (in the Stratonovich interpretation of the noise [10]). Thus the partition function

$$Z = \int \mathcal{D}(\{\hat{s}(\vec{x})\}) \Pi_{\vec{x}} [\delta(\hat{s}^2(\vec{x}) - 1)] e^{-E/k_B \tilde{T}} \tag{2}$$

achieved in the $t \to \infty$ limit incorporates the constraint that $|\hat{s}(\vec{x})| = 1$ for all $\vec{x}$.

From Eq. (2), one can see how $\tilde{T}_c$ inferred from numerical solutions of Eq. (1) depends on coarse graining. To do this, we first specialize to the following simple form for $E(\{\vec{S}\})$ in d space dimensions:

$$E(\{\vec{S}\}) = \frac{J}{2}\int d^d x(\nabla \hat{s}(\vec{x}))^2, \quad (3)$$

where J measures the exchange strength. Equation (2) is then the partition function of the nonlinear sigma model (NLσM) with three components of the field [7].

Aside from the high-wave number (short-distance) cutoff, Λ, this model has only one parameter—the dimensionless temperature $T \equiv k_B\tilde{T}/J\Lambda^{2-d}$. The model undergoes its phase transition when this parameter assumes a critical value, T_c. The RG equation describing the change of T as the NLσM is coarse grained by eliminating all Fourier components of $\vec{S}(\vec{x})$ whose wave numbers $\vec{q}$ exceed Λ/b (i.e., $\Lambda/b < |\vec{q}| \leq \Lambda$) has been calculated [7,8] as a double power series in T and $\epsilon \equiv d - 2$:

$$\partial T/\partial l = -\epsilon T + aT^2 + \cdots. \quad (4)$$

Here the positive constant $a = 1/2\pi$, b is a dimensionless scale factor greater than unity, and $l \equiv \ln(b)$.

For small T and ϵ, the terms explicitly displayed in (4) are the dominant ones. In fact these terms capture the qualitative physics of the model quite generally. Equation (4) has fixed points at $T = 0$, $T = \infty$, and $T = T^* \equiv \epsilon/a$, respectively controlling the low-temperature phase, the high-temperature phase, and the critical point. When the original microscopic value of T, viz., $T(l = 0)$, is $< T^*$ ($> T^*$), then $T(l) \to 0$ ($\to \infty$), as l increases, indicating that the system is in the low-T, ferromagnetic (high-T, paramagnetic) phase. Only when $T(0) = T^*$ does $T(l)$ remain fixed at T^*, meaning that the critical fixed point is unstable, and that T^* is in fact the dimensionless critical temperature, T_c: $T_c = 2\pi\epsilon + O(\epsilon^2)$ [7]. For any given values of b ($= e^l$) and $T(0)$, moreover, Eq. (4) allows one to calculate the dimensionless temperature $T(l)$ that produces, on the coarse-grained scale, static equilibrium properties equivalent to those of the starting microscopic problem with $l = 0$ and temperature $T(0)$.

Solving (4) for $T(l)$ yields the explicit result

$$T(l) = T_c/[1 + e^{\epsilon l}(T_c/T(0) - 1)]. \quad (5)$$

$T(l)$ and $T(0)$ correspond both at the low-temperature fixed point, $T(0) = 0$, and at the critical fixed point, $T(0) = T_c$. The unphysical divergence of $T(l)$ at a finite value of $T(0)$ in Eq. (5) results from our using at large T the small-T solution of Eq. (4). The true $T(l)$ increases monotonically with $T(0)$, diverging only at $T(0) = \infty$.

Compare now this coarse graining with those typically used in simulations of the LLG equations. Such simulations generally use variables that represent regions encompassing 10–30 spins on a side, so that $b \sim 10$–30. The rescaling of the exchange interactions, and hence of the reduced temperature, is typically carried out at the level of dimensional analysis, and omits the important corrections that come from the elimination of the high-wave vector modes. This amounts to truncating Eq. (4), which becomes $\partial T(l)/\partial l = -\epsilon T(l)$, yielding $T(l) = T(0)e^{-\epsilon l}$. In this case $T(l)$ reaches the critical temperature T_c only when $T(0) = T_c^0$, which exceeds T_c by the factor $e^{\epsilon l}$. Thus, this approximation overestimates the value of T_c by $e^{\epsilon l}$. For the physically relevant case of $\epsilon = 1$ and $l = 2.30$, T_c is overestimated by a factor of roughly 10, which is just the sort of error observed in practice [6].

This explains the order-of-magnitude errors in T_c inferred from micromagnetic simulations using block spins. Unfortunately, in practice the approximation $T_c = 2\pi\epsilon$ from Eq. (4) does not predict T_c accurately in the physically relevant case $\epsilon = 1$. If, as is almost always the case, however, acceptable experimental or numerical estimates of T_c for the material in question exist, then Eq. (5) with $\epsilon = 1$ can be used to provide a good approximation to $T(l)$, at least for $T(0)$'s not too much greater than T_c. This is illustrated in Fig. 1, which shows equilibrium magnetization (M) versus $\tilde{T}$ curves for a model Permalloy cube of size $(48\text{ nm})^3$, calculated from the 3D NLσM of Eq. (3), spatially discretized to give model (6) with applied field $\vec{H}_A = 0$. The block size was $(r = 3\text{ nm})^3$; other parameter values given below Eq. (8). The curves with square and oval symbols, respectively, result from choosing exchange constants $A = 9.63 \times 10^{-12}$ J/m, the rough, unrenormalized value for Permalloy, and $A(b) = (\tilde{T}/b\tilde{T}_c) \times [1 + b(\tilde{T}_c/\tilde{T} - 1)]A$, the renormalized value that follows from Eq. (5) with $\epsilon = 1$, $b = 10$ [the factor relating the single spin scale (~ 0.3 nm) to the 3 nm scale], and $\tilde{T}_c = 1000$ K, the rough Curie temperature for Permalloy. The former curve overestimates T_c by roughly the predicted factor $b = 10$, while the latter produces a very reasonable M vs $\tilde{T}$ curve.

Of course, micromagnetic simulations are more commonly used to study magnetic behavior not near criticality but for $k_B\tilde{T} \ll J\Lambda^{2-d}$. Here too, the block size of the calculation influences the result. For example, Fig. 2(a) shows M vs H_A curves computed for a model 2D magnetic slab with an energy function consisting of isotropic nearest neighbor exchange interactions and an applied field, $\vec{H}_A$. The slab has thickness a, and is divided up

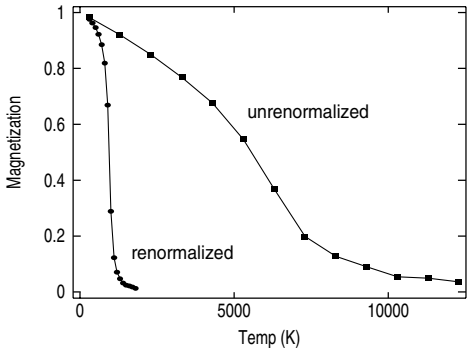

FIG. 1. M vs $\tilde{T}$ curves for the model Permalloy cube, from LLG Eq. (6), with parameters as given in text, and unrenormalized (square symbols) and renormalized (oval symbols) values of the exchange constant.

into a square lattice of blocks of dimension $r \times r \times a$, i.e., of volume $V = ar^2$. The magnetic moment of the ith block, $\vec{S}_i$, is $\vec{S}_i = M_s V \hat{s}_i$, where M_s is the saturation magnetization, and $\hat{s}_i$ a unit vector. Calculations were performed using the following spatially discretized version of Eq. (1), with open boundary conditions:

$$\partial \vec{S}_i(t)/\partial t = -\gamma \vec{S}_i \times \mu_0 \vec{H}_i^{\rm tot} - \alpha\gamma \hat{s}_i \times (\vec{S}_i \times \mu_0 \vec{H}_i^{\rm tot}) + \gamma \mu_0 \vec{S}_i \times \vec{\eta}_i. \quad (6)$$

Here the net field experienced by $\vec{S}_i$ is $\vec{H}_i^{\rm tot} = \vec{H}_A + \vec{H}_{\rm ex}$, where $\vec{H}_{\rm ex} = (2A/r^2 M_s \mu_0)\sum_j \hat{s}_j$, with A the exchange constant and $\sum_j$ a sum over blocks j that border i, and $\langle \vec{\eta}_i(t)\vec{\eta}_j(0)\rangle = D\vec{1}\,\delta_{i,j}\delta(t)$, with $D = 2k_B\tilde{T}\alpha/\gamma\mu_0^2 M_s V$; it follows [5,10] that as $t \to \infty$ the system achieves the equilibrium Boltzmann distribution at temperature $\tilde{T}$ for the energy function of the nearest neighbor Heisenberg model in an applied field:

$$E_{\rm Heis} = -J_H \sum_{\langle i,j\rangle} \hat{s}_i \cdot \hat{s}_j - \vec{H}_H \cdot \sum_i \hat{s}_i, \quad (7)$$

with $\sum_{\langle i,j\rangle}$ a sum on near-neighbor spin pairs, and

$$J_H \equiv 2Aa, \qquad H_H \equiv \mu_0 H_A M_s a r^2. \quad (8)$$

Shown in Fig. 2(a) are three equilibrium M vs H_A curves, computed from Eq. (6) at $\tilde{T} = 300°$ K with $a =$ 2 nm and block sizes: $r = 2$, 4, and 8 nm. In each case $\alpha = 0.1$, $A = 9.63 \times 10^{-12}$ J/m, $\mu_0 = 4\pi \times 10^{-7}$ H/m, $\mu_0 M_s = 1$ T, and the area of the slab is 64 nm $\times$ 64 nm.

A 4th order predictor-corrector method with a discrete time step of 5×10^{-14} s and typical equilibration times of 0.1 nsec was used. It is clear that the three results are systematically different, but unclear how they are connected to one another or to the true M vs H curves for the slab. To apply the RG to these questions, note that in Fourier space the exchange term of $E_{\rm Heis}$ is proportional to $\sum_{\vec{q}}(\sum_{i=x,y}\cos(q_i r))|\hat{s}(\vec{q})|^2$, where $\hat{s}(\vec{q})$ is the Fourier transform of $\hat{s}_i$. Writing $\cos(q_i r) \sim 1 - (q_i r)^2/2$, and approximating the square Brillouin zone of model (7) by a circle of radius $\Lambda \sim 1/r$ gives $E_{\rm Heis}$ the form of the 2D NLσM (3), with the high-momentum cutoff considered earlier, and an added applied field, $-\vec{H} \cdot \int d^2x \hat{s}(\vec{x})$.

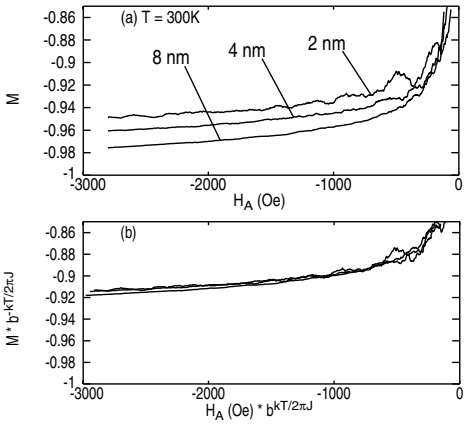

FIG. 2. M vs H_A data for $r = 2$, 4, and 8 nm blocks at 300°: (a) raw data; (b) data using RG scaling, as in text.

The equilibrium magnetization, $M(T, H)$, of this model, as a function of the dimensionless temperature T and field $h \equiv H/J\Lambda^2$, satisfies the RG equation [11]:

$$M(T, h) = \zeta(l) M(T(l), h(l)). \quad (9)$$

Neither the rescaling factor $\zeta(l)$ nor the l-dependent field and dimensionless temperature, $h(l)$ and $T(l)$ can be calculated exactly. However, in $d = 2 + \epsilon$ dimensions, they have, again, been calculated [7,8] in a double power series expansion in ϵ and T, with the result:

$$\zeta(l) = e^{-\int_0^l I(T(l'),h(l'))dl'}, \quad (10)$$

where $I(T, h) \equiv T/[2\pi(1 + h)]$, and $T(l)$ and $h(l)$ are determined by the differential equations

$$\begin{aligned} dT(l)/dl &= [-\epsilon + I(T(l), h(l))]T(l), \\ dh(l)/dl &= 2h(l), \end{aligned} \quad (11)$$

with the initial conditions $T(0) = T$ and $h(0) = h$.

In 2D, where $\epsilon = 0$, Eqs. (11) can be solved to yield

$$T(l) = T/[1 + TX(l)/4\pi], \qquad h(l) = he^{2l}; \quad (12)$$

here $X(l) \equiv \ln\{1 + he^{2l}/(1 + h)e^{2l}\}$. The scale factor $\zeta(l)$ in Eq. (10) is difficult to calculate exactly. However, in the often realistic limit where h and T are both small compared to unity, $X(l)$ reduces to $-2l + O(h)$, whereupon

$$\zeta(l) \to e^{-Tl/2\pi}\{1 + O[hT/2\pi, (T/2\pi)^2]\}. \quad (13)$$

In this limit, results (12) for fixed $\tilde{T}$ can be written $J(l) \sim J(0)e^{-k_B\tilde{T}l/2\pi J(0)}$ and $H(l) \sim H(0)e^{2l}e^{-k_B\tilde{T}l/2\pi J(0)}$.

This explains qualitatively why the raw M vs H_A curves shown in Fig. 2(a) look so different: In addition to omitting the $(\tilde{T}l)$-dependent corrections to J and H required to make the different calculations equivalent, the naive LLG computations omitted the scale factor $\zeta(l)$. To check that this works quantitatively, we recalculated from Eq. (6) the M vs H curves for block sizes $r = 4$ nm and $r = 8$ nm, using values of the exchange constant $A = A(l)$ related to the value, $A(0) = 9.63 \times 10^{-12}$ J/m, used at $r = 2$ nm, by $A(l) = A(0)e^{-k_B\tilde{T}l/2\pi J_H}$, for $l = \ln 2$ and $l = \ln 4$, respectively. These 4 and 8 nm magnetizations were then multiplied by the scale factors $\zeta(l) = e^{-k_B\tilde{T}l/2\pi J_H}$, and plotted against $e^{k_B\tilde{T}l/2\pi J_H}H_A$. The results for 4 nm ($l = \ln 2$) and 8 nm ($l = \ln 4$) are plotted along with the raw 2 nm data in Fig. 2(b). The three curves are essentially indistinguishable. Thus the RG does excellently in connecting micromagnetic data acquired with different block sizes in our simple model, despite the approximations involved in relating model (6) to the NLσM model, the fact that the quoted RG results are valid only in the

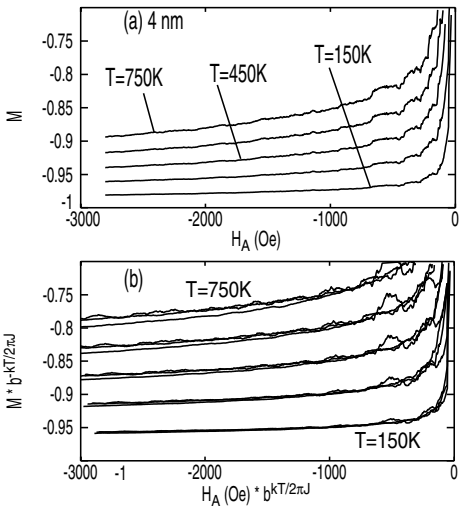

FIG. 3. (a) Raw M vs H_A data for $r = 4$ nm blocks at five equally spaced temperatures from 150° to 750°; (b) RG-scaled data for $r = 2$, 4, and 8 nm blocks, at the same five temperatures.

thermodynamic limit, and the approximate nature of the RG calculations themselves.

A large part of this success is that $x \equiv k_B\tilde{T}/2\pi J_H$, the small parameter for the low-T RG expansion, is indeed small at 300° for typical magnetic material, reflecting the high values of magnetic critical temperatures. For the parameters used here, $x \sim 0.016$. Moreover, even at 3000 Oe, the largest field studied here, $h \sim H_H/J_H \sim 10^{-3}$, so the approximation for $\zeta(l)$ in Eq. (13) is valid.

Figure 3 illustrates the effect of changing $\tilde{T}$. The upper panel shows raw M vs H_A data for $r = 4$ nm, for $\tilde{T}$'s between 150° and 750°, with all other parameters as in Fig. 2. The lower panel shows, for each $\tilde{T}$ value, three curves corresponding to $r = 2$, 4, and 8 nm, scaled according to the RG prescription. Though the RG predictions become less reliable as $\tilde{T}/\tilde{T}_c$ increases, the alignment of the three curves is respectable even at 750°.

Practical micromagnetic simulations involve not just Zeeman and exchange energies but anisotropy and dipolar terms. The renormalization of the coefficients of such terms can also be treated with the low-temperature expansion methods discussed here. The renormalization of anisotropy strength proceeds similarly [8] to that of an applied field. For example, addition to the NLσM in an applied z field of the easy uniaxial anisotropy energy, $-\frac{1}{2}\Delta \int d^dx s_z^2(\vec{x})$, replaces Eqs. (11) by

$$\begin{aligned} dT(l)/dl &= [-\epsilon + K(T(l), h(l), g(l))]T(l), \\ dh(l)/dl &= 2h(l), \\ dg(l)/dl &= [2 - 2K(T(l), h(l), g(l))]g(l), \end{aligned} \tag{14}$$

where $g \equiv \Delta/J\Lambda^2$, and $K(T, h, g) \equiv T/[2\pi(1 + h + g)]$. Finally, ζ, the scale factor for the magnetization in Eq. (10), becomes $\zeta(l) = e^{-\int_0^l K(T(l'),h(l'),g(l'))dl'}$.

In the simplest low-q approximation, dipolar interactions in the 2D NLσM can be written as the sum of a hard uniaxial anisotropy (demagnetizing) term, perpendicular to the sample, and a nonlocal quadratic term (with coefficient denoted u_d), involving only the components of the spins within the slab. For small u_d, u_d obeys the low-T RG equation $du_d(l)/dl = (1 - 2K(l))u_d(l)$ [12]. Generalizations to $d > 2$ and/or more realistic lattice models can be obtained by similar methods [12].

We conclude that, apart from being a numerical necessity, the discretization of the LLG equation embodies the elimination of small scale degrees of freedom and therefore contains important physics. For numerical micromagnetics in practical situations, it will be useful to develop approximate RG methods [13] that correspond more precisely to changing block sizes in the LL equation than does momentum shell RG, and that produce better approximations for T_c and other high-temperature properties than does the low-temperature RG discussed here. The principle that micromagnetic parameters cannot be chosen independent of numerical block size and the use of the RG as a prescription for choosing these parameters can be fruitfully incorporated into numerical endeavors.

[1] D. Weller and A. Moser, IEEE Trans. Magn. **35**, 4423 (1999).
[2] L. D. Landau and E. M. Lifshitz, Phys. Z. Sowjetunion **8**, 153 (1935).
[3] See, e.g., R. L Conger and F. C. Essig, Phys. Rev. **104**, 915 (1956).
[4] T. L. Gilbert, Phys. Rev. **100**, 1243 (1955).
[5] W. F. Brown, Phys. Rev. **130**, 1677 (1963).
[6] *Proceedings of the 44th Annual Conference on Magnetism and Magnetic Materials, San Jose, CA, 1999* [J. Appl. Phys. **87**, 6639 (2000)].
[7] See, e.g., E. Brézin and J. Zinn-Justin, Phys. Rev. Lett. **36**, 691 (1976); Phys. Rev. B **14**, 3110 (1976).
[8] D. R. Nelson and R. A. Pelcovits, Phys. Rev. B **16**, 2191 (1977).
[9] Implicitly assumed in Eq. (1) is a high-wave number (short-distance) cutoff to control ultraviolet divergences.
[10] Equation (1) reaches a stationary Boltzmann distribution only under the so-called "Stratonovich interpretation" [R. L. Stratonovich, SIAM J. Control **4**, 362 (1966)] of the "multiplicative" noise term.
[11] K. G. Wilson and J. Kogut, Phys. Rep. **12C**, 75 (1974).
[12] See, e.g., A. Aharony and M. E. Fisher, Phys. Rev. B **8**, 3323 (1973); R. A. Pelcovits and B. I. Halperin, Phys. Rev. B **19**, 4614 (1979).
[13] See, e.g., T. Niemeijer and J. M. J. van Leeuwen, Phys. Rev. Lett. **31**, 1411 (1973).